Atmos. Chem. Phys. Discuss., 14, 32667–32708, 2014
www.atmos-chem-phys-discuss.net/14/32667/2014/
doi:10.5194/acpd-14-32667-2014
© Author(s) 2014. CC Attribution 3.0 License.

Atmospheric Chemistry and Physics Discussions
Open Access

This discussion paper is/has been under review for the journal Atmospheric Chemistry and Physics (ACP). Please refer to the corresponding final paper in ACP if available.

The diurnal variation in stratospheric ozone from the MACC reanalysis, the ERA-Interim reanalysis, WACCM and Earth observation data: characteristics and intercomparison

A. Schanz[1], K. Hocke[1], N. Kämpfer[1], S. Chabrillat[2], A. Inness[3], M. Palm[4], J. Notholt[4], I. Boyd[5], A. Parrish[6], and Y. Kasai[7]

[1]Institute of Applied Physics and Oeschger Centre for Climate Change Research, University of Bern, Bern, Switzerland
[2]Belgium Institute of Space Aeronomy, Brussels, Belgium
[3]ECMWF, Reading, UK
[4]Institute of Environmental Physics, Universität Bremen, Bremen, Germany
[5]Contractor to BC Scientific, Consulting LLC, USA
[6]Department of Astronomy, University of Massachusetts, Amherst, MA, USA
[7]Department of Environmental Chemistry and Engineering, Tokyo Institute of Technology, Tokyo, Japan

Received: 6 October 2014 – Accepted: 9 December 2014 – Published: 22 December 2014

Correspondence to: A. Schanz (ansgar.schanz@iap.unibe.ch)

Published by Copernicus Publications on behalf of the European Geosciences Union.

ACPD
14, 32667–32708, 2014

Abstract

In this study we compare the diurnal variation in stratospheric ozone derived from free-running simulations of the Whole Atmosphere Community Climate Model (WACCM) and from reanalysis data of the atmospheric service MACC (Monitoring Atmospheric Composition and Climate) which both use a similar stratospheric chemistry module. We find good agreement between WACCM and the MACC reanalysis for the diurnal ozone variation in the high-latitude summer stratosphere based on photochemistry. In addition, we consult the ozone data product of the ERA-Interim reanalysis. The ERA-Interim reanalysis ozone system with its long-term ozone parametrization can not capture these diurnal variations in the upper stratosphere that are due to photochemistry. The good dynamics representations, however, reflects well dynamically induced ozone variations in the lower stratosphere. For the high-latitude winter stratosphere we describe a novel feature of diurnal variation in ozone where changes of up to 46.6 % (3.3 ppmv) occur in monthly mean data. For this effect good agreement between the ERA-Interim reanalysis and the MACC reanalysis suggest quite similar diurnal advection processes of ozone. The free-running WACCM model seriously underestimates the role of diurnal advection processes at the polar vortex at the two tested resolutions. The intercomparison of the MACC reanalysis and the ERA-Interim reanalysis demonstrates how global reanalyses can benefit from a chemical representation held by a chemical transport model. The MACC reanalysis provides an unprecedented description of the dynamics and photochemistry of the diurnal variation of stratospheric ozone which is of high interest for ozone trend analysis and research on atmospheric tides. We confirm the diurnal variation in ozone at 5 hPa by observations of the Superconducting Submillimeter-Wave Limb-Emission Sounder (SMILES) experiment and selected sites of the Network for Detection of Atmospheric Composition Change (NDACC). The latter give valuable insight even to diurnal variation of ozone in the polar winter stratosphere.

ACPD
14, 32667–32708, 2014

1 Introduction

Biases in satellite-based ozone trend analysis due to measurements at different local time and drifting satellite orbits renewed the interest in diurnal variations of stratospheric ozone (Bhartia et al., 2013). Model projections indicate a recovery of the ozone layer of about 1 % per decade (Jonsson et al., 2009; Garny et al., 2013; Chehade et al., 2013; Kyrölä et al., 2014; Gebhardt et al., 2014) while the diurnal variation in stratospheric ozone typically has an amplitude of 2–4 % which may induce a serious bias in trend estimates from satellite ozone measurements.

The diurnal variation in stratospheric ozone was researched by new studies based on chemistry–climate model simulations, ground-based microwave radiometry and satellite observations (e.g. Sakazaki et al., 2013; Studer et al., 2013a; Parrish et al., 2014). Schanz et al. (2014) investigated the global, seasonal and regional behaviour of diurnal variation in stratospheric ozone by means of the free-running chemistry–climate model WACCM. The study explained the basic underlying physical processes as temperature-dependent photochemical reactions within the Chapman cycle and the catalytic NO cycle which are the main contributors to the diurnal variation in stratospheric ozone. The strong connection to photochemistry in the stratosphere leads to a seasonality in diurnal ozone variation especially at high latitudes. The maximum ozone variation during a day is up to 0.8 ppmv (15 %) at the polar circle in summer in WACCM simulation (Schanz et al., 2014). This surprisingly strong amplitude is confirmed by ground-based microwave radiometer at Ny-Ålesund, Svalbard (Palm et al., 2013) and indicates that a correction of diurnal sampling effects in stratospheric ozone data sets is more needed than previously expected.

Sakazaki et al. (2013) compared the diurnal variation in stratospheric ozone from nudged chemistry–climate model simulations (SD-WACCM where SD stands for specified dynamics) to observations from the Superconducting Submillimeter-Wave Limb-Emission Sounder (SMILES, Kikuchi et al., 2013). The SMILES observations showed

ACPD
14, 32667–32708, 2014

CC BY

a good agreement in the tropics to SD-WACCM data (Sakazaki et al., 2013) where dynamics are nudged in the lower atmosphere.

Parrish et al. (2014) derived the diurnal variation in stratospheric ozone using 18 years of microwave radiometer measurements at Mauna Loa (Hawaii). They compared the observed results to simulations of the Goddard Earth Observing System Chemistry Climate Model (GEOSCCM, Duncan et al., 2007; Strahan et al., 2007; Oman et al., 2011) with two different implementations of atmospheric chemical processes. The observed and the simulated diurnal variation in stratospheric ozone agreed mostly within 1 % (2σ) of the estimated statistical errors. Studer et al. (2014) derived a climatology of the diurnal ozone variation using a 17 years series of stratospheric ozone profiles measured by a microwave radiometer at Bern, Switzerland. They found indications for an interannual variability of the diurnal ozone variation.

The good agreement of model data and observations may indicate that a model-assisted correction of diurnal sampling effects in satellite ozone measurements could be feasible. Alternatively to a model-assisted correction of satellite data, the assimilation of satellite ozone measurements into an advanced chemistry–climate model with two-way interactions between dynamics and atmospheric composition may be considered. The assimilating model system can incorporate the diurnal ozone variation in a correct manner. The Earth observation programme Copernicus of the EU develops such a chemistry–climate model system called Monitoring Atmospheric Composition and Climate (MACC). MACC assimilates satellite data of atmospheric composition, including ozone, into a global atmosphere model to provide a reanalysis of atmospheric composition for the years 2003–2012. Such a model system might help to correct diurnally sampled ozone data from biased satellite measurements and finally improve the quality of ozone trend estimates.

The present study follows on Schanz et al. (2014) and scrutinizes the WACCM results with the help of reanalysis data. The diurnal ozone variation from the MACC reanalysis, the ERA-Interim reanalysis and the WACCM model is intercompared and results are confirmed at 5 hPa by selected ground-based observations of the the Net-

ACPD
14, 32667–32708, 2014

CC BY

work for Detection of Atmospheric Composition Change (NDACC) and satellite-based observations of the Superconducting Submillimeter-Wave Limb-Emission Sounder (SMILES). Further, the study presents a remarkably strong diurnal variation based on advection at the polar regions in winter which is even stronger than the known effects based on photochemistry. This novel feature is discussed in a separated section by means of the potential vorticity distribution and an Arctic NDACC site.

The article is organized as follows: in Sect. 2 the different data sets from model systems and instruments are described. Section 3 intercompares the diurnal ozone variation derived from the MACC reanalysis, the ERA-Interim reanalysis, WACCM and NDACC instruments. Section 4 gives a brief summary of the results and concluding remarks.

2 Model systems and observations

2.1 MACC reanalysis system

The EU project Monitoring Atmospheric Composition and Climate (MACC) fosters a chemical weather forecast system which will be fed by the observations of the upcoming Sentinel satellites of the Copernicus Earth Observation programme. The global model and data assimilation system of MACC (Inness et al., 2013) is based on the European Centre for Medium-Range Weather Forecast's (ECMWF) integrated forecast system (IFS, Flemming et al., 2009; Stein et al., 2012). The representation of the atmospheric chemical system is held by a chemical transport model (CTM) which is coupled to the IFS via the OASIS4 coupler (Redler et al., 2010). That means the MACC reanalysis considers two-way interaction of dynamics and composition.

The coupled CTM is called Model of OZone And Related chemical Tracers (MOZART v3.5, Kinnison et al., 2007; Stein et al., 2012) and calculates chemical production and loss rates of the atmospheric gases. The implementation of Stein et al. (2012) used by the MACC reanalysis from 2009 onwards comprises 115 species, 71 photolysis reac-

ACPD
14, 32667–32708, 2014

tions, 223 gas phase reactions and 21 heterogeneous reactions. The MOZART model simulates tropospheric and stratospheric chemistry on a 1.125° by 1.125° horizontal grid. The vertical model domain is divided into 60 layers on hybrid–pressure ($\sigma - p$) coordinates (Phillips, 1957) with a model top at 0.1 hPa.

Satellite retrievals of reactive gases, aerosols and greenhouse gases are assimilated into the MACC reanalysis system by a four-dimensional variational (4-D-VAR) data assimilation system (Talagrand and Courtier, 1987; Courtier et al., 1994; Courtier, 1997). Stratospheric ozone data are assimilated from different satellite-based instruments e.g. Global Ozone Monitoring Experiment (GOME), Michelson Interferometer for Passive Atmospheric Sounding (MIPAS), Microwave Limb Sounder (MLS), Ozone Monitoring Instrument (OMI), Solar Backscatter UltraViolet Instrument (SBUV/2), Scanning Imaging Absorption Spectrometer for Atmospheric CHartographY (SCIAMACHY). For further information on the assimilation of ozone data we refer to Inness et al. (2013). Aside the meteorological variables the MACC system calculates forecasts of reactive gases including ozone (O_3), carbon monoxide (CO), nitrogen oxides (NO_x) and formaldehyde (HCHO), aerosols and greenhouse gases.

Data records, monitored present state, forecasts and reanalysis of atmospheric composition are provided by the MACC project (atmosphere.copernicus.eu). The MACC reanalysis ozone product contains 6 hourly analysis data (forecast data is available every 3 h) at 00:00, 06:00, 12:00 and 18:00 UT and is available from 2003 to 2012. Inness et al. (2013) found that stratospheric ozone from the MACC reanalysis agrees to within ±10 % in most seasons and regions which is considerably better compared to the free-running CTM MOZART.

2.2 ERA-Interim reanalysis

The ERA-Interim reanalysis is a global atmospheric reanalysis produced by the ECMWF. The ERA-Interim project aimed at establishing an improved reanalysis by approaching the existing problems of ERA-40's hydrological cycle, stratospheric circulation and temporal consistence of atmospheric fields (Dee et al., 2011).

ACPD
14, 32667–32708, 2014

The prognostic ozone system of the ERA-Interim reanalysis is a simplified, built-in chemistry routine. Ozone follows a scheme of linear relaxation to a local photochemical equilibrium which is calculated by a two-dimensional photochemical model. The coefficients of the ozone parametrisation are given as a function of latitude, model level, and month, hence there is no diurnal variation or longitudinal variation (Geer et al., 2007). That means the ERA-Interim reanalysis does not represent a fully two-way interactive coupling of dynamics and composition and it can not model the diurnal ozone cycle in the upper stratosphere that is due to photochemistry. The prognostic ozone system was upgraded following Cariolle and Teyssèdre (2007) who improved the representation of polar ozone destruction by taking into account local stratospheric temperature and the total chlorine content. The upgraded ozone system reproduced well the inter-annual variability related to temperature in polar vortices. For more details on the ozone system of the ERA-Interim reanalysis we refer to Cariolle and Déqué (1986) and Cariolle and Teyssèdre (2007).

The ERA-Interim reanalysis uses a 4-D-VAR data assimilation system (Rabier et al., 2000; Dee et al., 2011). The atmospheric model performs simulations on hybrid-pressure ($\sigma - p$) coordinates (Phillips, 1957) with a model top at 0.1 hPa. Reanalysis data of ERA-Interim are available in 6 hourly data at 00:00, 06:00, 12:00 and 18:00 UT from 1979 onwards. Ozone data from the ERA-Interim reanalysis are often used in atmospheric research (e.g. Goncharenko et al., 2012; Hocke et al., 2013; Studer et al., 2013a). The quality of ERA-Interim ozone data was assessed by Dragani (2011) who found that ERA-Interim reanalysis is in better agreement than the ERA-40 equivalent compared to a total column ozone reference. In the stratosphere the ERA-Interim reanalysis shows mean residuals of about ±10 % compared to satellite observations (Dragani, 2011).

2.3 WACCM

The Whole Atmosphere Community Climate Model (WACCM) is a fully coupled chemistry–climate model which simulates the entirety of the Earth's atmosphere. The

ACPD
14, 32667–32708, 2014

WACCM model was developed by the National Center of Atmospheric Research (NCAR) (Garcia et al., 2007; Marsh et al., 2007; Tilmes et al., 2007) and is embedded into the software framework of the Community Earth System Model (CESM) which comprises a land, ice, ocean and an atmosphere model. The atmosphere is simulated from the Earth's surface up to the lower thermosphere at 5.1×10^{-6} hPa (~ 150 km).

In the present article, WACCM version 4 was utilized with the preconfigured, free-running F 2000 scenario which reflects a perpetual year with atmospheric conditions corresponding to the year 2000. Free-running means that the model is not influenced by effects of data assimilation or nudging.

The chemical representation of the atmosphere is based on the stratospheric chemistry of the CTM MOZART (v3, Kinnison et al., 2007) which comprises the main production and loss processes of 59 atmospheric species. In addition, the WACCM model simulates chemical heating, gravity wave drag, molecular diffusion and ionization. The ozone distribution calculated by the model feeds back to the model dynamics.

The simulations are carried out on a horizontal resolution of 1.9° latitude by 2.5° longitude and a vertical fragmentation of 66 layers on hybrid-pressure ($\sigma - p$) coordinates (Phillips, 1957) which are terrain-following below the 100 hPa level and isobar above. The resolution of the vertical coordinates ranges from 1.1 to 2.0 km in the middle atmosphere. The time steps of the atmosphere and land model were reduced to 15 min in order to achieve good results for the diurnal variability of stratospheric composition. The global output data set of WACCM has a time resolution of 1 h and is derived from a one year simulation starting at 1 January 00:00 UT.

An overview on the model systems of the MACC reanalysis, the ERA-Interim reanalysis and WACCM is given in Table 1.

2.4 SMILES climatology

The SMILES (Kikuchi et al., 2013) was jointly operated by the Japan Aerospace Exploration Agency (JAXA) and National Institute of Communication Technology (NICT) at the Japanese Experiment Module on the International Space Station (ISS). The

ACPD
14, 32667–32708, 2014

SMILES experiment was launched to space on 9 September 2009 and had been observing the atmosphere from 12 October 2009 until 21 April 2010 when an instrument component failed.

During seven months in operation SMILES has been observing profiles of atmospheric minor constituents such as O_3 (and isotopes), HCl, ClO, HO_2, BrO, HNO_3. The SMILES observations cover a latitudinal range mostly within 38° S to 65° N (exceptions occur when the ISS was turned) with a vertical resolution of 3.5–4.1 km.

The relatively low inclination of the ISS supports the study of diurnal variations of ozone, minor constituents, ozone isotopes, rate constants and atmospheric tides (e.g. Sakazaki et al., 2012, 2013; Sato et al., 2014; Kuribayashi et al., 2014) by means of the SMILES observations. Kreyling et al. (2013) derived a climatology of stratospheric and mesospheric trace gases and temperature from SMILES observations. The ozone climatology of Kreyling et al. (2013) is distributed via the NICT SMILES website (http://smiles.nict.go.jp/index-e.html). Due to irregular spatial and temporal distribution of the SMILES data, the ozone climatology was obtained by binning the ozone measurements of SMILES within latitude bands (20–40° S, 20° S–20° N, 20–50° N and 50–65° N) and over bimonthly periods.

2.5 GROMOS measurements

The GROund-based Millimeter-wave Ozone Spectrometer (GROMOS) is situated at the Bern NDACC site, Switzerland (46°57′ N, 7°26′ E) and has been operating since 1994 (Dumitru et el., 2006). In the present study ozone profiles are used with a time resolution of 30 min which have been measured with the Fast Fourier transform (FFT) spectrometer of GROMOS. Ozone profiles are retrieved at fixed pressure levels from about 0.2 to 50 hPa with a vertical resolution of approximately 10 km. A climatology of diurnal variation in mesospheric and stratospheric ozone was derived for the period from 1994 to 2011 by Studer et al. (2014). For further details on the GROMOS climatology we refer to the latter study.

ACPD
14, 32667–32708, 2014

Ozone profiles from GROMOS are regularly used for satellite validations or for studies on middle-atmospheric dynamics, diurnal ozone variation and sudden stratospheric warmings (Hocke et al., 2007, 2013; Flury et al., 2009; Studer et al., 2014).

2.6 MLO ozone measurements

The Mauna Loa Observatory (MLO, 19.5° N, 204.5° E) is a tropical NDACC site sensing ozone profiles. The MLO microwave radiometer has been operating since 1995 at an elevation of 3400 m where the quality of sensed profiles benefits from a low zenith tropospheric opacity (Parrish et al., 2014). Ozone profiles are retrieved from 20–65 km with a vertical resolution from 6–14 km. Technical details of the MLO microwave radiometer are described by Parrish et al. (1992).

The diurnal variation of ozone was studied by Parrish et al. (2014) from reprocessed measurements with hourly time resolution of the profiling MLO radiometer. They compared the results to measurements of space-based microwave limb sounders (e.g. SMILES) and the solar backscattered instruments of SBUV/2 and found very small differences of less than 1.5 % amongst the profiles.

2.7 OZORAM measurements

The OZOne Radiometer for Atmospheric Measurements (OZORAM) is deployed to Ny-Ålesund, Svalbard in the high Arctic (78.9° N, 11.9° E). The instrument is operated by the Alfred Wegener Institute (AWI) and the University of Bremen, Germany in the frame of NDACC. Since 2008 OZORAM has been observing ozone profiles of the middle atmosphere from 30–70 km with an altitude resolution of 10–20 km and time intervals of 1 h.

Palm et al. (2010) compared stratospheric ozone observations from OZORAM to satellite-based instruments such as EOS-MLS and TIMED and found good agreement within 10 %. For further information on the technical details, the ozone retrieval and the quality of ozone measurements we refer to Palm et al. (2010).

ACPD
14, 32667–32708, 2014

Ground-based microwave radiometers such as GROMOS, OZORAM and the MLO microwave radiometer measure ozone profiles from approximately 25–70 km at day- and nighttime with the same quality so that the determination of the small diurnal cycle of stratospheric ozone is possible. For further details on the retrieval technique of the microwave instruments we refer to Rodgers (2000).

3 Results and discussion

3.1 Intercomparison with respect to ground- and satellite-based measurements

Diurnal ozone variation of model systems and selected NDACC sites are intercompared at the 5 hPa level where satellite ozone trend analysis is most biased by sampling effects. Further, strongest diurnal variation in ozone appears mostly from 3–5 hPa, little above the ozone maximum (VMR) and hence at the peak of the stratospheric ozone layer (Bhartia et al., 2013; Parrish et al., 2014; Sakazaki et al., 2013).

By sorting and binning of all ozone values of a month according to the local time, we get monthly mean ozone as function of local time ($O_{3,m}(LT)$) showing the mean diurnal variation in stratospheric ozone. The relative, diurnal ozone variation is calculated with respect to monthly mean ozone at midnight

$$\Delta O_3(LT) = \frac{O_{3,m}(LT) - O_{3,m}(00{:}00)}{O_{3,m}(00{:}00)}. \quad (1)$$

Figure 1 displays mean March (2012) diurnal variations in stratospheric ozone over NDACC sites at northern midlatitudes (upper panel) and tropics (bottom panel) according to Eq. (1). The figure compares data from two microwave radiometers (dashed and solid gray lines), the WACCM model (blue line), the MACC reanalysis (red markers) and the ERA-Interim reanalysis (black markers). In Fig. 1, diurnal ozone variation at 5 hPa features three different characteristics during a day: almost constant ozone over nighttime (WACCM, MLO radiometer), a morning minimum and an afternoon maximum.

ACPD
14, 32667–32708, 2014

CC BY

Table 2 compares the morning minima and afternoon maxima of the different data sets from model systems and microwave radiometers. Figure 1 and Table 2 clearly show that the ERA-Interim reanalysis only renders a small diurnal variation in ozone of approximately 0.8 %. This result reveals that the simplified, linear ozone representation of the ERA-Interim reanalysis does not adequately reflect diurnal variation in ozone.

There is agreement between the microwave radiometers, WACCM and the MACC reanalysis in spring (Fig. 1a and b) though the temporal resolution of the MACC reanalysis is rather coarse. At 19:00 LT the ozone VMR values from the MACC reanalysis are beyond the data of the WACCM model and the ground-based microwave radiometers over Mauna Loa and Bern. The low temporal resolution of the MACC reanalysis might cause minor defects in strength of the diurnal variation in ozone. Further defects might be related to the chemical data of the CTM of the MACC reanalysis which is coupled every hour only. The MACC project also provides 3 hourly forecast data which we considered to be not adapted for intercomparison to the ERA-Interim reanalysis or the WACCM model. Nevertheless, the 6 hourly reanalysis data of the MACC project is already valuable for the study of the diurnal ozone variation on a global scale.

Further, Fig. 1 includes the SMILES climatology (orange line) for midlatitudes (zonal mean from 20 to 50° N) and tropics (zonal mean from 20° S to 20° N) which is available for the bimonthly period of March–April only. Over Bern, Switzerland, the SMILES climatology agrees with the morning minimum and the afternoon maximum of WACCM and the MACC reanalysis (see Table 2), whereas over Mauna Loa, Hawaii only the WACCM model and the MLO microwave radiometer are mutually consistent.

Over Mauna Loa, Hawaii there is only qualitative agreement of the SMILES climatology and all data from model systems and the MLO microwave radiometer. Kreyling et al. (2013) compiled the SMILES climatology by sampling bimonthly zonal mean profiles from non-sun-synchronous orbits, thus from all local times. The apparent discrepancy of SMILES over the Mauna Loa NDACC site (Fig. 1b) may be related to the irregular data sampling due to the ISS orbit which accounts of up to 20 % (relative error) in the SMILES climatology product (Kreyling et al., 2013). Such discrepancies and the

ACPD
14, 32667–32708, 2014

phase bias in the diurnal ozone variation from ground-based measurements, WACCM, the MACC reanalysis and the SMILES climatology (see Fig. 1) remind that our present understanding of ozone photochemistry in the stratosphere is still incomplete (Crutzen and Schmailzl, 1983).

3.2 Intercomparison of the model systems

The strength of the diurnal variation in ozone is represented by the peak-to-valley difference D_{O_3} which is defined by Eq. (2) for each grid point where $O_{3,max}$ refers to the maximum, $O_{3,min}$ to the minimum ozone VMR during a day (00:00 to 24:00 UT).

$$D_{O_3} = O_{3,max} - O_{3,min} \quad (2)$$

D_{O_3} is the interval width of the ozone values of a day and depends on the amplitudes of the diurnal and subdiurnal variations without any information about timing. Further, we often discuss monthly means of relative diurnal variation $D_{O_3,m}/O_{3,m}$ where $D_{O_3,m}$ and $O_{3,m}$ are the monthly means at a gridpoint.

Figure 2 shows zonal-mean $D_{O_3,m}/O_{3,m}$ for March, June, September and December of 2012 as derived from the MACC reanalysis. The strengths of the diurnal ozone variation in Fig. 2 is presented for the pressure range from 1 to 50 hPa and all latitudes. Figure 2a and c displays diurnal ozone variation of more than 6.0 % (0.6 ppmv) above the 3 hPa pressure level in the tropics and below the 20 hPa pressure level in March and September. The diurnal variation of ozone in the upper stratosphere is based on photochemistry (cf. Fig. 1) and hence is a function of latitude. The diurnal variation from the MACC reanalysis in the lower, tropical stratosphere is mostly based on O_x transport related to vertical tidal winds and the strong vertical ozone gradient in the lower stratosphere as described by Sakazaki et al. (2013).

A further feature in March and September (Fig. 2a and c) are enhancements of $D_{O_3,m}/O_{3,m}$ in the Arctic and Antarctic upper stratosphere of more than 15 % (1.0 ppmv) which are clearly separated from the tropical enhancement. These features are due to dynamics at the Arctic and Antarctic and relate to advection effects. Aside these

ACPD
14, 32667–32708, 2014

CC BY

maxima the MACC reanalysis shows also minima of diurnal ozone variation in March and September (Fig. 2a and c) of approximately 1.5 % (0.3 ppmv) at 10 hPa near the equator.

In the MACC reanalysis data, the diurnal variation of stratospheric ozone is enhanced in June and December (Fig. 2b, d) at the Arctic and Antarctic polar circles (marked as magenta dashed lines). For instance, in Fig. 2b and d, the MACC reanalysis shows high values of diurnal ozone variation in the respective summer hemisphere of up to 16.9 % (1.3 ppmv) between the 2 and 5 hPa pressure levels at the polar circle. This feature is based on the long sunshine duration at the polar circle in summer where ozone is accumulated during daytime to very high values. The MACC reanalysis accurately renders this feature of the stratospheric daily ozone cycle and assures its strength of reflecting photochemical induced diurnal ozone variation.

However, the global maximum in diurnal ozone variation in June (Fig. 2b) from the MACC reanalysis appears around 2 hPa in the Antarctic polar region and is approximately 46.6 % (3.3 ppmv) which is a surprisingly high value. The Arctic and Antarctic stratosphere in winter is a dynamically dominated region and most of the diurnal ozone variation relates to advection at different time scales. The MACC reanalysis captures the diurnal ozone variation from different origins as photochemistry and dynamics and gives an unprecedented global picture.

In a similar manner, Figs. 3 and 4 show zonal-mean $D_{O_3,m}/O_{3,m}$ for March, June, September and December as derived from simulations of the WACCM model and from the ERA-Interim reanalysis. With regard to the intercomparison to the MACC reanalysis and the ERA-Interim reanalysis the hourly WACCM output was down-sampled to a 6 hourly temporal resolution.

In the WACCM simulation, diurnal variation of stratospheric ozone is maximal in June and December at the polar circle of the summer hemisphere in between the 1 and 5 hPa pressure levels. This strong photochemical features of up to approximately 18.6 % (0.9 ppmv) can be clearly seen in Fig. 3b and d and are consistent to the results of the MACC reanalysis.

ACPD
14, 32667–32708, 2014

From the 2 to 5 hPa pressure level where photochemistry is important, the simulated diurnal variation in ozone of WACCM is weaker than at the polar circles in summer. For instance, in March and September as shown in Fig. 3a and c the strength of the daily ozone cycle is approximately 5 %. Exceptions are maxima of diurnal ozone variation at 2 hPa and 80° latitude in the respective autumn hemisphere in Fig. 3a and c. These exceptions are artifacts of the strong diurnal variation due to photochemistry in summer.

Compared to the MACC reanalysis, the WACCM model underestimates all dynamically induced effects such as the diurnal ozone variation at the Arctic and Antarctic and in the lower, tropical stratosphere. The WACCM model shows strong effects of diurnal ozone variation only above 10 hPa which mostly are based on photochemistry. This strongly indicates that the free-running WACCM model underestimates tidal winds in the lower stratosphere which could be also due to the low horizontal resolution. Further, advection processes at diurnal and shorter time scales in the polar regions in winter are not adequately reflected in the WACCM simulation. On the other hand, WACCM and the MACC reanalysis are mutually consistent with diurnal ozone variation based on photochemistry.

The ERA-Interim reanalysis does not consider locally time-dependent ozone photochemistry and hence can not render the strong diurnal ozone variation due to photochemistry at the polar circle in summer (Fig. 4b, d). The ERA-Interim reanalysis shows this feature at 2 hPa polewards of the polar circles with only 8.4 % (0.3 ppmv). At this point, the limit of the simplified, linear ozone system of the ERA-Interim reanalysis becomes evident. Unsurprisingly, the ERA-Interim ozone system can not keep up with the fully coupled CTMs of the MACC reanalysis and the WACCM model.

In the Arctic and Antarctic winter stratosphere the ERA-Interim reanalysis and the MACC reanalysis benefit from their strong dynamics assimilation systems. Such systems give a good representation of the diurnal ozone variation due to advection processes. For instance, the ERA-Interim reanalysis shows a maximum in diurnal ozone variation in June (Fig. 4b) at around 1 hPa of approximately 30.5 % (1.0 ppmv). This

ACPD
14, 32667–32708, 2014

feature can also be seen to a similar extent in the MACC reanalysis (Fig. 2b). The ERA-Interim reanalysis nicely reflects the diurnal variation of ozone based on advection in the polar region in winter but also in the lower, tropical stratosphere.

Figure 5 gives a comprehensive overview of the diurnal ozone variations in the MACC reanalysis, the ERA-Interim reanalysis and WACCM at 5 hPa. It is evident that neither WACCM nor the ERA-Interim reanalysis can match all of the important characteristics which figure in the MACC reanalysis. WACCM fails in the polar winter stratosphere where the ERA-Interim reanalysis agrees well with the MACC reanalysis. The ERA-Interim reanalysis fails in the polar summer stratosphere where WACCM agrees well with MACC. Especially, WACCM and the MACC reanalysis show the strong diurnal ozone variation at the polar circle of approximately 0.8 ppmv (15 %) in summer and in addition agree well on the seasonal timing of this feature. Contours in Fig. 5 depict the sunshine duration (dashed lines) and the solar zenith angle (solid lines) which govern the seasonal pattern of the photochemically induced diurnal variation.

The three model systems show different features of the diurnal variation in ozone based on their specific model composition. Eventually, it has been the weaknesses in photochemistry or short term advection of WACCM and the ERA-Interim reanalysis which revealed the different origins of the diurnal ozone variation in the stratosphere. The MACC reanalysis combines the strengths of both and therefore gives an unprecedented global picture on diurnal ozone variation in the stratosphere.

3.3 The influence of horizontal resolution on WACCM simulations

The analysis of diurnal variation of ozone in the dynamically dominated polar region in winter by WACCM questions the influence of horizontal resolution on the simulation results. In Sect. 3.2 results from WACCM were presented at medium horizontal resolution of 1.9° latitude by 2.5° longitude. Here, the term "medium" is with respect to the higher horizontal resolution of the MACC reanalysis (T255 truncation with about 0.7° horizontal resolution; Inness et al., 2013). Diurnal variation of the stratospheric composition in the polar winter region depends on the quality of the dynamical representation

ACPD
14, 32667–32708, 2014

in the model. This in turn highly depends on the implemented interaction processes of the atmospheric layers as tidal waves, planetary waves, gravity waves and atmospheric instabilities such as sudden stratospheric warmings.

In order to test a different horizontal resolution of WACCM, a simulation was performed at the lower 4° latitude by 5° longitude resolution. Figure 6 exemplifies the relative difference in ozone VMR from 18:00 to 06:00 UT relative to ozone VMR at 06:00 UT at 5 hPa for the low and the medium horizontal resolution. The figure presents a representative day of the Southern Hemisphere in winter. From Fig. 6 it can be deduced that simulated diurnal variation depends on the horizontal resolution in the following way: higher horizontal resolution results in enhanced diurnal variation in ozone at the polar region in winter.

This result is in line with Richter et al. (2008) who showed that the gravity wave parameterization at different horizontal resolutions of WACCM results in different variability in the stratosphere. That means, whenever dynamics at diurnal and shorter timescales in the stratosphere are simulated with WACCM, it is important to consider the actual potential of the model. For instance, at the polar circle the medium resolution is approximately 113 by 86 km which can solve many but not for all the gravity waves in the atmosphere. For internally-generated gravity waves without a gravity wave parameterization, simulations need to be performed at high horizontal and vertical resolution (e.g. T213 grid with about 60 km horizontal resolution and 300 m vertical resolution, Sato et al., 2009).

From the results of Sect. 3.2 and different results of the two horizontal resolutions (Fig. 6) it is inferred that neither the low nor the medium horizontal resolution of WACCM can represent the features of diurnal variation in the polar winter region. WACCM with its internal gravity wave parametrization is tuned to model adequate mean flows and jets in the middle atmosphere and the simulation of diurnal variation in the polar region in winter overstresses the prospects of the model.

ACPD
14, 32667–32708, 2014

3.4 Diurnal variation in the polar regions

The surprisingly strong diurnal variation in the polar regions is accessible by one of the NDACC's instruments. The OZORAM microwave radiometer located at Ny-Ålesund, Svalbard (78.9° N, 11.9° E) observes diurnally sampled ozone profiles at such high latitudes in summer and winter.

Figure 7 presents the mean diurnal ozone variation observed by the OZORAM microwave radiometer in June 2011 at 5 hPa along with the corresponding data of the MACC reanalysis and the ERA-Interim reanalysis. The figure shows the relative diurnal variation according to Eq. (1). The diurnal ozone variation in Fig. 7 is based on photochemistry and is up to approximately 8 % for the WACCM model and the OZORAM radiometer which are almost perfectly consistent. The MACC reanalysis shows even stronger diurnal variation in ozone of up to 10 %.

Figure 8 shows diurnal ozone variation from OZORAM measurements during two periods: 21–26 June 2011 and 1–6 December 2012. The figure presents the ozone time series of OZORAM per mean ozone of the two periods, respectively. The MACC reanalysis and OZORAM measurements agree well (mostly within the error range of OZORAM) during the summer period in June 2011 (Fig. 8a). Again, the diurnal ozone variation is based on photochemistry and shows similar characteristics as in Fig. 7. Figures 7 and 8a confirm the strong diurnal ozone variations around the polar circle in summer which form in the MACC reanalysis and in the independent observations of the OZORAM microwave radiometer. However, the MACC reanalysis and OZORAM microwave radiometer show poor agreement in ozone VMR (the MACC reanalysis shows up to 60 % more ozone VMR during the presented period).

The bottom panel of Fig. 8 displays OZORAM measurement in December 2012. The OZORAM measurement and the MACC reanalysis show qualitative agreement mostly within the error range of the radiometer data. The diurnal ozone variation is superposed by variability at longer and sub-diurnal time scales. Thus, the dynamically dominated polar region in winter shows no clear diurnal signature in ozone variability at 5 hPa.

ACPD
14, 32667–32708, 2014

A view on the diurnal ozone variation in the Arctic and Antarctic is presented in Fig. 9 from WACCM, the MACC reanalysis and ERA-Interim reanalysis. The relative difference in ozone VMR from 18:00 to 06:00 UT relative to ozone VMR at 06:00 UT is shown at 5 hPa for 21 June 2012. WACCM is shown for the corresponding day of the simulation. The WACCM model and the MACC reanalysis agree well in the Northern Hemisphere (summer) where photochemistry is dominating the diurnal ozone variation (Fig. 9a and b). In the Southern Hemisphere (winter) WACCM seems to fail in simulating vortex dynamics and related advection compared to the MACC reanalysis (cf. Fig. 9d, e). On the other hand, the ERA-Interim reanalysis agrees well with the MACC reanalysis in the polar region in winter (Southern Hemisphere, Fig. 9b, c) but does not reflect the diurnal ozone variation based on photochemistry in the polar region in summer (Northern Hemisphere, Fig. 9e, f).

Dynamics of the polar vortices and related advection cause strong, aperiodic ozone variation in the polar region in winter. A useful quantity for studying synoptic variability of polar vortices is potential vorticity or shorter PV. Potential vorticity is often used to analyze vortex dynamics (e.g. Kew et al., 2009). The observed structure, the understanding of vortex dynamics and the benefits of potential vorticity are reviewed by Waugh and Polvani (2010).

When potential vorticity is conserved, an air parcel moves along its potential vorticity isopleth. Further, it is assumed that the change of the ozone VMR in the air parcel is negligible over the period of a day in the polar winter stratosphere. Thus a diurnal change in the potential vorticity isopleth would indicate a diurnal change in the trajectory which is associated to a diurnal change in ozone at a fixed geographic location (Danielson, 1961; McIntyre and Palmer, 1983; Coffey et al., 1999; McWilliams et al., 2003). Such colocated variations in potential vorticity and ozone indicate diurnal variation in ozone based on vortex dynamics.

The difference in potential vorticity in Fig. 10 is determined as the difference from 18:00 to 06:00 UT from the ERA-Interim reanalysis. The Antarctic polar vortex in Fig. 10 shows stronger changes in potential vorticity than the midlatitudes and tropics. These

ACPD
14, 32667–32708, 2014

CC BY

strong changes in potential vorticity correlate to ozone variability at the same time scale in Fig. 9e and f. This connection confirms that transport processes related to the dynamics of the stratospheric polar vortex evoke the strong diurnal ozone variation in the polar winter.

The polar vortices in the stratosphere show day-to-day variability which manifest in elongation of the vortices and displacement from the poles (Waugh and Polvani, 2010). Tides and periodic gravity wave flux perturb the stratospheric vortex. The perturbed vortex forms vortex Rossby waves with typical spiral band structures of zonal wavenumber 2. Partly, these structures are visible in Fig. 10. To confirm the interconnection of gravity waves to diurnal ozone variation in the polar region in winter further research based on highly resolved data is needed (e.g. ECMWF-T799, Yamashita et al., 2010).

4 Conclusions

The intercomparison of diurnal variation in ozone from reanalysis and chemistry–climate modelling shows a wide range of agreements but also differing features. For instance, the strong diurnal variation in ozone at the polar circle in summer as derived from the MACC reanalysis suites the global pattern of seasonality in diurnal ozone variation of the WACCM model. Diurnal variation in stratospheric ozone is mostly based on ozone accumulation due to the Chapman cycle over day time which is not entirely balanced by catalytic ozone depletion. The ERA-Interim reanalysis with its linearized, two-dimensional photochemical ozone model does not reflect such diurnal variation of stratospheric ozone based on photochemistry.

Differences also appear in the winter stratosphere where the free-running WACCM model shows less diurnal variation than the MACC reanalysis and the ERA-Interim reanalysis. These variations depend to some extent on horizontal resolution of the free-running WACCM model where higher resolutions show more variability. However, WACCM at either low and the medium resolution tends to underestimate the diurnal variation of ozone in winter at high latitudes which are most likely based on vortex dy-

ACPD
14, 32667–32708, 2014

namics and related advection. Such variation occurs in the MACC reanalysis data and is up to 47 % in the upper stratosphere. The ECMWF ERA-Interim reanalysis confirms the large amplitudes of diurnal and subdiurnal variation in ozone at the stratospheric polar vortex. From analysis of the potential vorticity structure we relate these effects to diurnal and subdiurnal vortex Rossby waves. Here, the present conception and understanding of diurnal ozone variation in the stratosphere is widened by the novelty of this surprisingly strong diurnal variation in the polar winter stratosphere.

In addition, the comparison to ECMWF's ERA-Interim and WACCM substantiates the benefits of a coupled CTM as in the MACC reanalysis system for the representation of the diurnal variation in stratospheric ozone. Our intercomparison study indicates the potential of the MACC reanalysis for an accurate description of the advection and the photochemical effects on the diurnal variation of stratospheric ozone while the ERA Interim reanalysis and free-running WACCM either fail for the photochemical effects or the diurnal advection effects.

The results show how gathering and preparation of data by the affiliated ground stations of the NDACC network yields additional value for atmospheric research and validation of the MACC reanalysis model system. Ground-based microwave radiometry is an important observation method for diurnal variation of stratospheric ozone. Partly, it was possible to validate the different model systems by NDACC observations. Therefore, further measurements of diurnal ozone variation in the polar regions as performed by Palm et al. (2013) are desirable to confirm and study the behaviour of diurnal variation in ozone at different seasons in Arctic and Antarctic. For instance, the recent start-up of the campaign instrument GROMOS-C (Fernandez et al., 2014) makes polar stratospheric ozone and its diurnal variation more accessible to ground-based microwave radiometry and could extend the global sampling of local ozone profiles. In addition, microwave instruments might benefit from reanalysis data with higher temporal resolution in order to validate and improve retrievals which focus on subdiurnal time scales.

ACPD
14, 32667–32708, 2014

Interesting results emerged from simulations at different horizontal resolutions of the WACCM model. In dynamically dominated regions as the polar night region, ozone variation at diurnal and shorter time scales depends on an accurate representation of dynamics at short time scales. This in turn is based on the implementation of atmospheric processes which interact between the atmospheric layers such as gravity waves, 2-days waves and sudden stratospheric warmings. We suspect that also other chemistry–climate models may have similar weaknesses and advised application to such short time scales is recommended.

Despite a suboptimal temporal resolution, the MACC reanalysis system impressively showed dynamical and photochemical features of diurnal variation in ozone at all latitudes and seasons. On this account, such a model system of chemical data integration and assimilated dynamics shows great promise for preprocessing diurnally sampled ozone data from space-borne instruments and correct potential biases in ozone trends. The diurnally sampled observations might be assimilated and reanalyzed with a coupled chemical transport model under consideration of a higher temporal resolution.

Acknowledgements. The research leading to these results has received funding from the European Community's Seventh Framework Programme ([FP7/2007–2013]) under grant agreement no. 284421 (see Article II.30. of the Grant Agreement). We acknowledge the MACC-II consortium, ECMWF for access to the ERA-Interim reanalysis data, the International Space Science Institute at Bern, Switzerland (ISSI Team #246, Characterizing Diurnal Variations of Ozone for Improving Ozone Trend Estimates, http://www.issibern.ch/teams/ozonetrend/) and the MeteoSwiss project MIMAH in the frame of GAW. Further, we thank L. Moreira Méndez for consultations on GROMOS data. The OZORAM measurements at the AWIPEV research base have been supported by the AWI Bremerhaven and the 'Deutsche Forschungsgemeinschaft' (DFG) in the projects NO 404/5-1, NO 404/5-2, NO 404/5-3.

ACPD
14, 32667–32708, 2014

References

Bhartia, P. K., McPeters, R. D., Flynn, L. E., Taylor, S., Kramarova, N. A., Frith, S., Fisher, B., and DeLand, M.: Solar Backscatter UV (SBUV) total ozone and profile algorithm, Atmos. Meas. Tech., 6, 2533–2548, doi:10.5194/amt-6-2533-2013, 2013. 32670, 32678

Cariolle, D. and Déqué, M.: Southern Hemisphere medium-scale waves and total ozone disturbances in a spectral General Circulation model, J. Geophys. Res., 91, 10825–10846, doi:10.1029/JD091iD10p10825, 1986. 32674

Cariolle, D. and Teyssèdre, H.: A revised linear ozone photochemistry parameterization for use in transport and general circulation models: multi-annual simulations, Atmos. Chem. Phys., 7, 2183–2196, doi:10.5194/acp-7-2183-2007, 2007. 32674, 32697

Chehade, W., Weber, M., and Burrows, J. P.: Total ozone trends and variability during 1979–2012 from merged data sets of various satellites, Atmos. Chem. Phys., 14, 7059–7074, doi:10.5194/acp-14-7059-2014, 2014. 32670

Coffey, M. T., Mankin, W. G., and Hannigan, J. W.: A reconstructed view of polar stratospheric chemistry, J. Geophys. Res., 104, 8296–8316, doi:10.1029/1998JD100045, 1999. 32686

Courtier, P.: Dual formulation of four-dimensional variational assimilation, Q. J. Roy. Meteor. Soc., 123, 2449–2461, 1997. 32673

Courtier, P., Thépaut, J.-N., and Hollingsworth, A.: A strategy for operational implementation of 4-D-Var, using an incremental approach, Q. J. Roy. Meteor. Soc., 120, 1367–1388, 1994. 32673

Crutzen, P. J. and Schmailzl, U.: Chemical budgets of the stratosphere, Planet. Space Sci., 31, 1009–1032, doi:10.1016/0032-0633(83)90092-2, 1983. 32680

Danielsen, E. F.: Trajectories: isobaroc, isentropic, and actual, J. Meteorol., 18, 479–486, 1961. 32686

Dee, D. P., Uppala, S. M, Simmons, A. J., Berrisford, P., Poli, P., Kobayashi, S., Andrae, U., Balmaseda, M. A., Balsamo, G., Bauer, P., Bechtold, P., Beljaars, A. C. M., van de Berg, L., Bidlot, J., Bormann, N., Delsol, C., Dragani, R., Fuentes, M., Geer, A. J., Haimberger, L., Healy, S. B., Hersbach, H., Hólm, E. V., Isaksen, L., Kållberg, P., Köhler, M., Matricardi, M., McNally, A. P., Monge-Sanz, B. M., Morcrette, J.-J., Park, B.-K., Peubey, C., de Rosnay, P., Tavolato, C., Thépaut, J.-N., and Vitartm, F.: The ERA-Interim reanalysis: confiduration and performance of the data assimilation system, Q. J. Royal Meteor. Soc., 137, 553–597, doi:10.1002/qj.828, 2011. 32673, 32674, 32697

ACPD
14, 32667–32708, 2014

Dragani, R.: On the quality of the ERA-Interim ozone reanalyses: comparisons with satellite data, Q. J. Roy. Meteor. Soc., 127, 1312–1326, doi:10.1002/qj.821, 2011. 32674, 32697

Dumitru, M. C., Hocke, K., Kämpfer, N., and Calisesi, Y: Comparison and validation studies related to ground-based microwave observations of ozone in the stratosphere and mesosphere, J. Atmos. Sol.-Terr. Phy., 68, 745–756, doi:10.1016/j.jastp.2005.11.001, 2006. 32676

Duncan, B. N., Strahan, S. E., Yoshida, Y., Steenrod, S. D., and Livesey, N.: Model study of the cross-tropopause transport of biomass burning pollution, Atmos. Chem. Phys., 7, 3713–3736, doi:10.5194/acp-7-3713-2007, 2007. 32671

Fernandez, S., Murk, A., and Kämpfer, N.: Design and characterization of a peltier-cold calibration target for a 110-GHz radiometer, IEEE T. Geosci Remote, 53, 344–351, doi:10.1109/TGRS.2014.2322336, 2014. 32688

Flemming, J., Inness, A., Flentje, H., Huijnen, V., Moinat, P., Schultz, M. G., and Stein, O.: Coupling global chemistry transport models to ECMWF's integrated forecast system, Geosci. Model Dev., 2, 253–265, doi:10.5194/gmd-2-253-2009, 2009. 32672

Flury, T., Hocke, K., Haefele, A., Kämpfer, N., and Lehmann, R.: Ozone depletion, water vapor increase, and PSC generation at midlatitudes by the 2008 major stratospheric warming, J. Geophys. Res., 114, D18302, doi:10.1029/2009JD011940, 2009. 32677

Garcia, R. R., Marsh, D. R., Kinnison, D. E., Boville, B. A., and Sassi, F.: Simulation of secular trends in the middle atmosphere, 1950–2003, J. Geophys. Res., 112, D09301, doi:10.1029/2006JD007485, 2007. 32675, 32697

Garny, H., Bodeker, G. E., Smale, D., Dameris, M., and Grewe, V.: Drivers of hemispheric differences in return dates of mid-latitude stratospheric ozone to historical levels, Atmos. Chem. Phys., 13, 7279–7300, doi:10.5194/acp-13-7279-2013, 2013. 32670

Gebhardt, C., Rozanov, A., Hommel, R., Weber, M., Bovensmann, H., Burrows, J. P., Degenstein, D., Froidevaux, L., and Thompson, A. M.: Stratospheric ozone trends and variability as seen by SCIAMACHY from 2002 to 2012, Atmos. Chem. Phys., 14, 831–846, doi:10.5194/acp-14-831-2014, 2014. 32670

Geer, A. J., Lahoz, W. A., Jackson, D. R., Cariolle, D., and McCormack, J. P.: Evaluation of linear ozone photochemistry parametrizations in a stratosphere-troposphere data assimilation system, Atmos. Chem. Phys., 7, 939–959, doi:10.5194/acp-7-939-2007, 2007. 32674

Goncharenko, L. P., Coster, A. J., Plumb, R. A., and Domeisen, D. I. V.: The potential role of stratospheric ozone in the stratosphere-ionosphere coupling during stratospheric warmings, Geophys. Res. Lett., 39, L08101, doi:10.1029/2012GL051261, 2012. 32674

ACPD
14, 32667–32708, 2014

Haefele, A., Hocke, K., Kämpfer, N., Keckhut, P., Marchand, M., Bekki, S., Morel, B., Egorova, T., and Rozanov, E.: Diurnal changes in middle atmospheric H_20 and O_3: observations in the alpine region and climate models, J. Geophys. Res., 113, D17303, doi:10.1029/2008JD009892, 2008.

Hocke, K., Kämpfer, N., Ruffieux, D., Froidevaux, L., Parrish, A., Boyd, I., von Clarmann, T., Steck, T., Timofeyev, Y. M., Polyakov, A. V., and Kyrölä, E.: Comparison and synergy of stratospheric ozone measurements by satellite limb sounders and the ground-based microwave radiometer SOMORA, Atmos. Chem. Phys., 7, 4117–4131, doi:10.5194/acp-7-4117-2007, 2007. 32677

Hocke, K., Studer, S., Martius, O., Scheiben, D., and Kämpfer, N.: A 20-day period standing oscillation in the northern winter stratosphere, Ann. Geophys., 31, 755–764, doi:10.5194/angeo-31-755-2013, 2013. 32674, 32677

Inness, A., Baier, F., Benedetti, A., Bouarar, I., Chabrillat, S., Clark, H., Clerbaux, C., Coheur, P., Engelen, R. J., Errera, Q., Flemming, J., George, M., Granier, C., Hadji-Lazaro, J., Huijnen, V., Hurtmans, D., Jones, L., Kaiser, J. W., Kapsomenakis, J., Lefever, K., Leitão, J., Razinger, M., Richter, A., Schultz, M. G., Simmons, A. J., Suttie, M., Stein, O., Thépaut, J.-N., Thouret, V., Vrekoussis, M., Zerefos, C., and the MACC team: The MACC reanalysis: an 8 yr data set of atmospheric composition, Atmos. Chem. Phys., 13, 4073–4109, doi:10.5194/acp-13-4073-2013, 2013. 32672, 32673, 32683, 32697

Jonsson, A. I., Fomichev, V. I., and Shepherd, T. G.: The effect of nonlinearity in CO_2 heating rates on the attribution of stratospheric ozone and temperature changes, Atmos. Chem. Phys., 9, 8447–8452, doi:10.5194/acp-9-8447-2009, 2009. 32670

Kew, S. F., Sprenger, M., and Davies, H. C.: Potential vorticity anomalies of the lowermost stratosphere: a 10-yr winter climatology, Mon. Weather Rev., 138, 1234–1249, doi:10.1175/2009MWR3193.1, 2009. 32686

Kikuchi, K., Nishibori, T., Ochiai, S., Ozeki, H., Irimajiri, Y., Kasai, Y., Koike, M., Manabe, T., Mizukoshi, K., Murayama, Y., Nagahama, T., Sano, T., Sato, R., Seta, M., Takahashi, C., Takayanagi, M., Masuko, H., Inatani, J., Suzuki, M., and Shiotani, M.: Overview and early results of the Superconducting Submillimeter-Wave Limb-Emission Sounder (SMILES), J. Geophys. Res., 115, D23, doi:10.1029/2010JD014379, 2013. 32670, 32675

Kinnison, D. E., Brasseur, G. P., Walters, S., Garcia, R. R., Marsh, D. R., Sassi, F., Harvey, V. L., Randall, C. E., Emmons, L., Lamarque, J. F., Hess, P., Orlando, J. J., Tie, X. X., Randel, W., Pan, L. L., Gettelman, A., Granier, C., Diehl, T., Niemeier, U., and Simmons, A. J.: Sensi-

tivity of chemical tracers to meteorological parameters in the MOZART-3 chemical transport model, J. Geophys. Res., 112, D20302, doi:10.1029/2006JD007879, 2007. 32672, 32675

Kreyling, D., Sagawa, H., Wohltmann, I., Lehmann, R., and Kasai, Y.: SMILES zonal and diurnal variation climatology of stratospheric and mesospheric trace gasses: O_3, HCl, HNO_3, ClO, BrO, HOCl, HO_2, and temperature, J. Geophys. Res., 118, 11888–11903, doi:10.1002/2012JD019420, 2013. 32676, 32679

Kuribayashi, K., Sagawa, H., Lehmann, R., Sato, T. O., and Kasai, Y.: Direct estimation of the rate constant of the reaction $ClO + HO_2 \rightarrow HOCl + O_2$ from SMILES atmospheric observations, Atmos. Chem. Phys., 14, 255–266, doi:10.5194/acp-14-255-2014, 2014. 32676

Kyrölä, E., Laine, M., Sofieva, V., Tamminen, J., Päivärinta, S.-M., Tukiainen, S., Zawodny, J., and Thomason, L.: Combined SAGE II–GOMOS ozone profile data set for 1984–2011 and trend analysis of the vertical distribution of ozone, Atmos. Chem. Phys., 13, 10645–10658, doi:10.5194/acp-13-10645-2013, 2013. 32670

Marsh, D. R., Garcia, R. R., Kinnison, D. E., Boville, B. A., Walters, S., Matthes, K., and Solomon, S. C.: Modeling the whole atmosphere response to solar cycle changes in radiative and geomagnetic forcing, J. Geophys. Res., 112, D23306, doi:10.1029/2006JD008306, 2007. 32675, 32697

McIntyre, M. E. and Palmer, T., N.: Breaking planetary waves in the stratosphere, Nature, 305, 593–600, doi:10.1038/305593a0, 1983. 32686

McWilliams, J. C., Graves, L. P., and Montgomery, M. T.: A formal theory for vortex Rossby waves and vortex evolution, Geophys. Astro. Fluid, 97, 275–309, doi:10.1080/0309192031000108698, 2003. 32686

Oman, L. D., Ziemke, J. R., Douglass, A. R., Waugh, D. W., Lang, C., Rodriguez, J. M., and Nielson, J. E.: The response of tropical tropospheric ozone to ENSO, Geophys. Res. Lett., 38, L13706, doi:10.1029/2011GL047865, 2011. 32671

Palm, M., Hoffmann, C. G., Golchert, S. H. W., and Notholt, J.: The ground-based MW radiometer OZORAM on Spitsbergen – description and status of stratospheric and mesospheric O_3-measurements, Atmos. Meas. Tech., 3, 1533–1545, doi:10.5194/amt-3-1533-2010, 2010. 32677

Palm, M., Golchert, S. H. W., Sinnhuber, M., Hochschild, G., and Notholt, J.: Influence of solar radiation on the diurnal and seasonal variability of O_3 and H_2O in the stratosphere and lower mesosphere, based on continuous observations in the tropics and the high arctic, in: Climate and Weather of the Sun-Earth System (CAWSES), Springer Atmospheric Sciences

ACPD
14, 32667–32708, 2014

Publisher: Springer Netherlands, 125–147, doi:10.1007/978-94-007-4348-9_8, 2013. 32670, 32688

Parrish, A., Connor, B. J., Tsou, J. J., McDermid, I. S., and Chu, W. P.: Ground-based microwave monitoring of stratospheric ozone, J. Geophys. Res., 97, 2541–2546, doi:10.1029/91JD02914, 1992. 32677

Parrish, A., Boyd, I. S., Nedoluha, G. E., Bhartia, P. K., Frith, S. M., Kramarova, N. A., Connor, B. J., Bodeker, G. E., Froidevaux, L., Shiotani, M., and Sakazaki, T.: Diurnal variations of stratospheric ozone measured by ground-based microwave remote sensing at the Mauna Loa NDACC site: measurement validation and GEOSCCM model comparison, Atmos. Chem. Phys., 14, 7255–7272, doi:10.5194/acp-14-7255-2014, 2014. 32670, 32671, 32677, 32678

Phillips, N. A.: A coordinate system having some special advantages for numerical forecasting, J. Meteorol., 14, 184–185, 1957. 32673, 32674, 32675

Rabier, F., Järvinen, H., Klinker, E., Mahfouf, J.-F., and Simmons, A.: The ECMWF operational implementation of four-dimensional variational assimilation. I: Experimental results with simplified physics, Q. J. Roy. Meter. Soc., 126, 1143–1170, doi:10.1002/qj.49712656415, 2000. 32674

Redler, R., Valcke, S., and Ritzdorf, H.: OASIS4 – a coupling software for next generation earth system modelling, Geosci. Model Dev., 3, 87–104, doi:10.5194/gmd-3-87-2010, 2010. 32672

Richter, J. H., Sassi, F., Garcia, R. R., Matthes, K., and Fischer, C. A.: Dynamics of the middle atmosphere as simulated by the Whole Atmosphere Community Climate Model, version 3 (WACCM3), J. Geophys. Res., 113, D08101, doi:10.1029/2007JD009269, 2008. 32684

Rodgers, C. D.: Inverse Methods for Atmospheric Sounding, World Scientific Publishing Co. Pte. Ltd., Singapore, 2000. 32678

Sakazaki, T., Fujiwara, M., Zhang, X., Hagan, M. E., and Forbes, J. M.: Diurnal tides from the troposphere to the lower mesosphere as deduced from TIMED/SABER satellite data and six global reanalysis data sets, J. Geophys. Res., 117, D13108, doi:10.1029/2011JD017117, 2012. 32676

Sakazaki, T., Fujiwara, M., Mitsuda, C., Imai, K., Manago, N., Naito, Y., Nakamura, T., Akiyoshi, H., Kinnison, D., Sano, T., Suzuki, M., and Shiotani, M.: Diurnal ozone variations in the stratosphere revealed in observations from the Superconducting Submillimeter-Wave Limb-Emission Sounder (SMILES) on board the International Space Station (ISS), J. Geophys. Res., 118, 1–16, doi:10.1002/jgrd.50220, 2013. 32670, 32671, 32676, 32678, 32680

Sato, K., Watanabe, S., Kawatani, Y., Tomikawa, Y., Miyazaki, K., and Takahashi, M.: On the origin of mesospheric gravity waves, Geophys. Res. Lett., 36, L19801, doi:10.1029/2009GL039908, 2009. 32684

Sato, T. O., Sagawa, H., Yoshida, N., and Kasai, Y.: Vertical profile of δ^{18}OOO from the middle stratosphere to lower mesosphere from SMILES spectra, Atmos. Meas. Tech., 7, 941–958, doi:10.5194/amt-7-941-2014, 2014. 32676

Schanz, A., Hocke, K., and Kämpfer, N.: Daily ozone cycle in the stratosphere: global, regional and seasonal behaviour modelled with the Whole Atmosphere Community Climate Model, Atmos. Chem. Phys., 14, 7645–7663, doi:10.5194/acp-14-7645-2014, 2014. 32670, 32671

Stein, O., Flemming, J., Inness, A., Kaiser, J. W., Schultz, M. G.: Global reactive gases forecast and reanalysis in the MACC project, J. Integr. Envi. Sci., 9, Supplement 1, 57–70, doi:10.1080/1943815X.2012.696545, 2012. 32672

Strahan, S. E., Duncan, B. N., and Hoor, P.: Observationally derived transport diagnostics for the lowermost stratosphere and their application to the GMI chemistry and transport model, Atmos. Chem. Phys., 7, 2435–2445, doi:10.5194/acp-7-2435-2007, 2007. 32671

Studer, S., Hocke, K., Pastel, M., Godin-Beekmann, S., and Kämpfer, N.: Intercomparison of stratospheric ozone profiles for the assessment of the upgraded GROMOS radiometer at Bern, Atmos. Meas. Tech. Discuss., 6, 6097–6146, doi:10.5194/amtd-6-6097-2013, 2013. 32670, 32674

Studer, S., Hocke, K., Schanz, A., Schmidt, H., and Kämpfer, N.: A climatology of the diurnal variations in stratospheric and mesospheric ozone over Bern, Switzerland, Atmos. Chem. Phys., 14, 5905–5919, doi:10.5194/acp-14-5905-2014, 2014. 32671, 32676, 32677

Talagrand, O. and Courtier, P.: Variational assimilation of meteorological observations with the adjoint vorticity equation, Q. J. Roy. Meteor. Soc., 113, 1311–1328, doi:10.1002/qj.49711347812, 1987. 32673

Tilmes, S., Kinnison, D. E., Garcia, R. R., Müller, R., Sassi, F., Marsh, D. R., and Boville, B. A.: Evaluation of heterogeneous processes in the polar lower stratosphere in the Whole Atmosphere Community Climate Model, J. Geophys. Res., 112, D24301, doi:10.1029/2006JD008334, 2007. 32675

Waugh, D. W. and Polvani, L. M.: Stratospheric polar vortices, Geoph. Monog. Series, 190, 43–57, doi:10.1029/2009GM000887, 2010. 32686, 32687

ACPD
14, 32667–32708, 2014

Yamashita, C., Liu, H.-L., and Chu, X.: Gravity wave variation during the 2009 stratospheric sudden warming as revealed by ECMWF-T799 and observations, Geophys. Res. Lett., 37, L22806, doi:10.1029/2010GL045437, 2010. 32687

ACPD
14, 32667–32708, 2014

Table 1. Overview on the implementation, data assimilation and resolution of the WACCM, the MACC reanalysis and ERA-Interim reanalysis model systems.

		WACCM	MACC reanalysis	ERA-Interim reanalysis
	model type	Global Circulation-Chemistry Model (free-running)	Chemical Weather Forecast System	Weather Forecast System
	model range	global, 0–140 km	global, 0–65 km	global, 0–65 km
	coupling	chemistry $\overset{\text{online}}{\longleftrightarrow}$ dynamics	chemistry $\overset{\text{60 min}}{\longleftrightarrow}$ dynamics	humidity $\overset{\text{30 min}}{\longleftrightarrow}$ dynamics ozone $\overset{\text{30 min}}{\longleftarrow}$ dynamics
Dynamics				
	resolution	1.9° lat × 2.5° lon, 66 lev	T255: 0.7° lat × 0.7° lon, 60 lev	T255: 0.7° lat × 0.7° lon, 60 lev
	time step	15 min	IFS: 30 min	IFS: 30 min
	assimilation	–	4-D-VAR (12 h); $\boldsymbol{v}$, p, T	4-D-VAR (12 h); $\boldsymbol{v}$, p, T
Chemistry				
	model	3-D MOZART (stratosphere)	3-D MOZART (tropo- and stratosphere)	linearized 2-D photochemical model, (lat-alt, no daily cycle)
	resolution	same as Dynamics	T159: 1.125° lat × 1.125° lon, 60 lev	same as Dynamics
Ozone				
	assimilation	–	4-D-VAR (12 h); gases, aerosols tropo- and stratosphere	4-D-VAR (12 h); O_3, humidity tropo- and stratosphere
	sources	–	e.g. GOME, MIPAS, MLS,...	e.g. GOME, MIPAS, MLS,...
	references	Garcia et al. (2007) Marsh et al. (2007)	Inness et al. (2013)	Dee et al. (2011); Dragani (2011) Cariolle and Teyssèdre (2007)

ACPD
14, 32667–32708, 2014

Table 2. Forming of the morning minimum and the afternoon maximum for a mean day of March from model systems and the Mauna Loa and Bern microwave radiometers (MWRs) (morning minimum/afternoon maximum in percent).

Data set	Bern, Switzerland	Mauna Loa, Hawaii
MACC	−0.8/3.2 %	–/5.2 %
ERA-Interim	–/0.8 %	–/–
WACCM	−0.8/1.9 %	−0.7/2.5 %
MWRs	–/2.4 %	−0.7/2.6 %
SMILES	–/3.8 %	−1.7/6.9 %

ACPD
14, 32667–32708, 2014

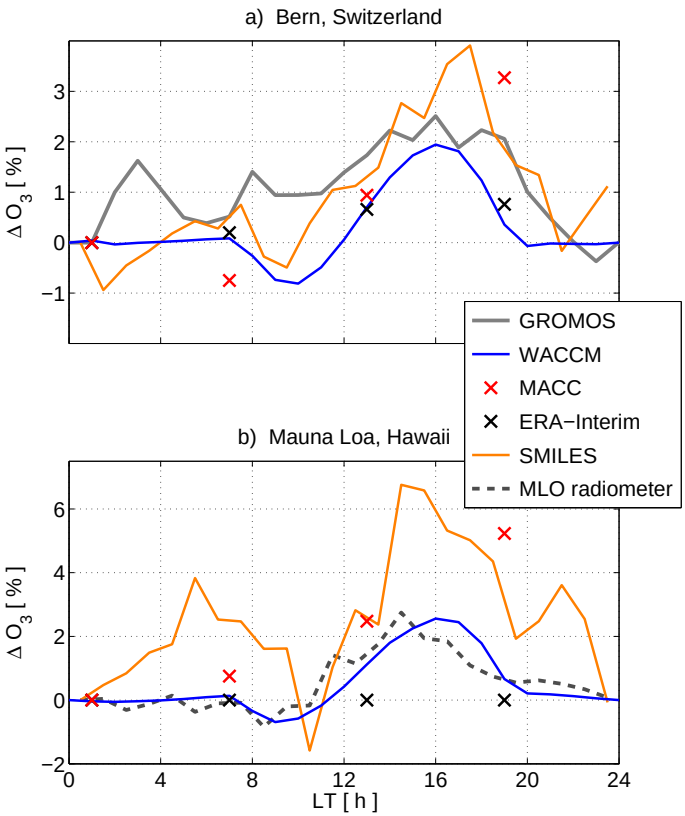

Figure 1. Relative diurnal variation in ozone from WACCM, the MACC reanalysis and the ERA-Interim reanalysis at 5 hPa over Mauna Loa, Hawaii (19.5° N, 204.5° E) and Bern, Switzerland (46°57′ N, 7°26′ E) for March 2012. The figures show the relative diurnal variation according to Eq. (1). The SMILES climatology (orange line) is taken for a similar period (March–April) but from 20–50° N for Bern and from 20° S–20° N for Hawaii.

ACPD
14, 32667–32708, 2014

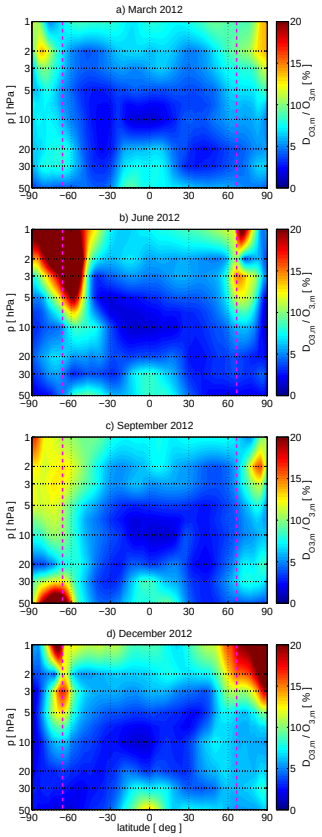

Figure 2. Zonal-mean $D_{O_3,m}/O_{3,m}$ derived from the MACC reanalysis. The figure shows monthly means in the middle and upper stratosphere for March, June, September and December of 2012 (according to Eq. 2, ff). The dashed, magenta lines refer to the polar circles.

ACPD
14, 32667–32708, 2014

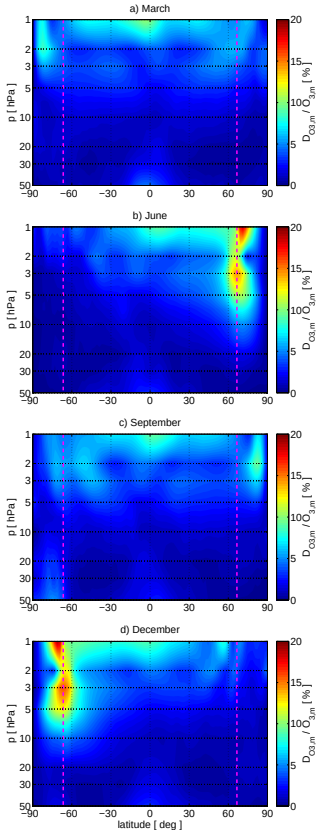

Figure 3. Same as Fig. 2 but derived from the WACCM model.

ACPD
14, 32667–32708, 2014

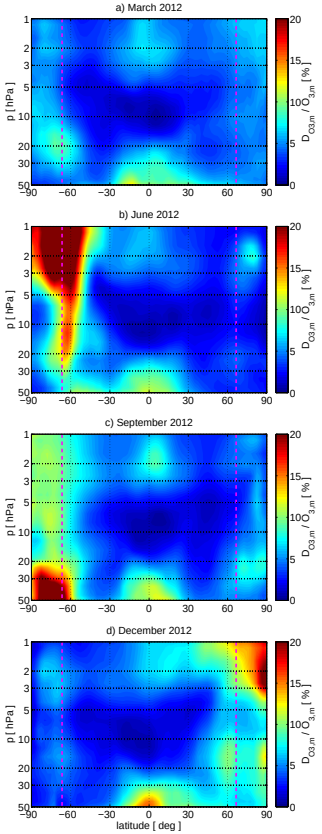

Figure 4. Same as Fig. 2 but derived from the ERA-Interim reanalysis of the year 2012.

ACPD
14, 32667–32708, 2014

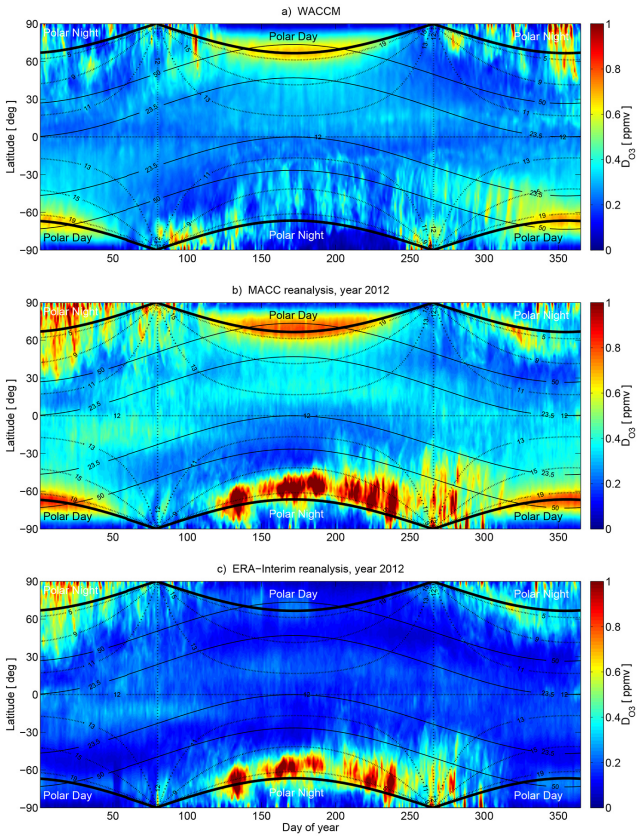

Figure 5. Seasonal behaviour of zonal-mean D_{O_3} (see Eq. 2) at 5 hPa derived from WACCM **(a)**, the MACC reanalysis **(b)** and the ERA-Interim reanalysis **(c)** (both from 2012). The solid contour lines refer to the solar zenith angle at noon. Dashed contour lines show the sunshine duration given in hours.

ACPD
14, 32667–32708, 2014

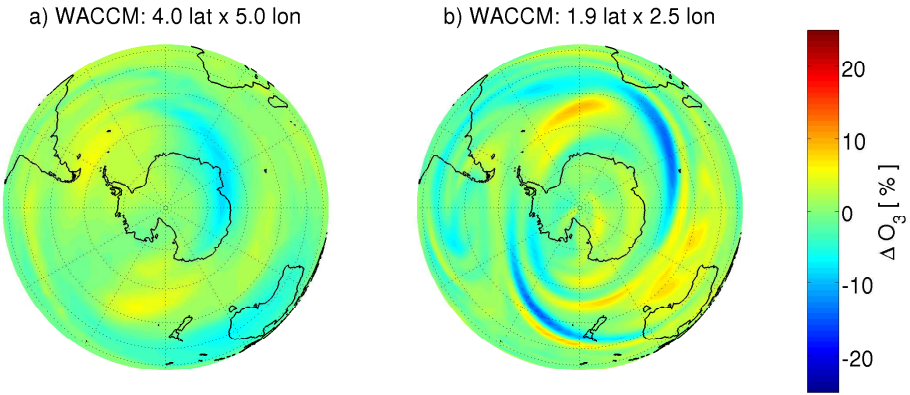

Figure 6. Relative difference in ozone VMR from 18:00 to 06:00 UT per ozone VMR at 06:00 UT. This difference is displayed at the 5 hPa pressure level for low **(a)** and medium resolution **(b)** of WACCM.

ACPD
14, 32667–32708, 2014

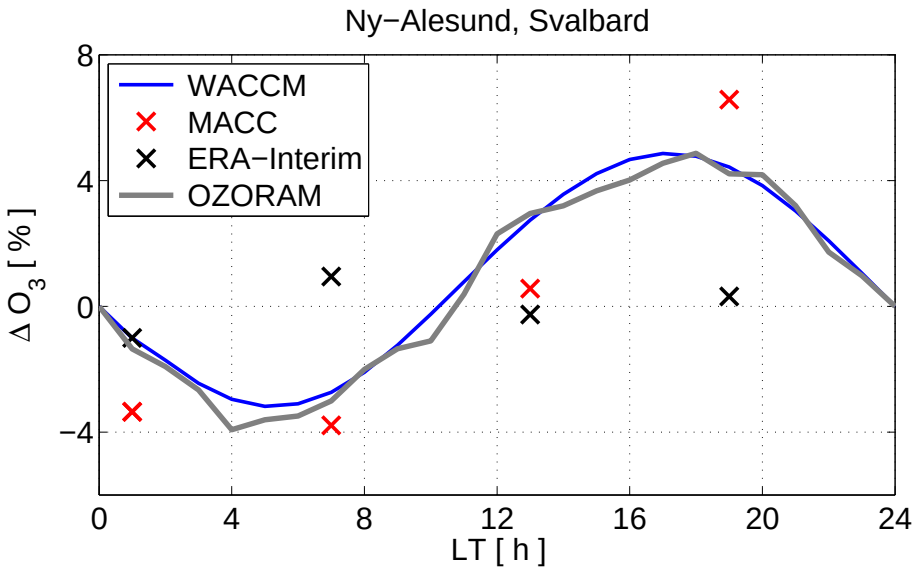

Figure 7. Relative diurnal variation in ozone from WACCM (blue line), the MACC reanalysis (red markers), the ERA-Interim reanalysis (black markers) and from the OZORAM radiometer (gray line) at 5 hPa over Ny-Ålesund, Svalbard (78.9° N, 11.9° E). The figure shows the relative diurnal variation according to Eq. (1). The SMILES climatology does not cover the high latitude of Ny-Ålesund.

ACPD
14, 32667–32708, 2014

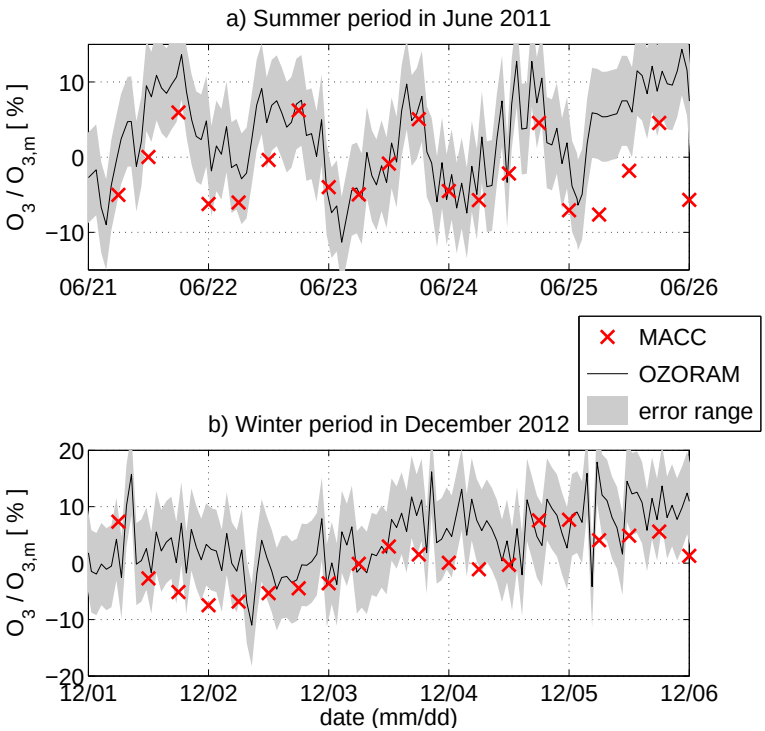

Figure 8. Relative diurnal variation in ozone from the MACC reanalysis and the OZORAM radiometer at 5 hPa over Ny-Ålesund, Svalbard (78.9° N, 11.9° E) for a summer **(a)** and a winter **(b)** period (21–26 June 2011 and 1–6 December 2012). The figure shows the ozone time series of OZORAM per mean ozone $O_{3,m}$ of the two periods, respectively. The summer period is taken from 2011 due to technical problems of the instrument in summer 2012. The uncertainty range stands for the combined random and systematic SD.

ACPD
14, 32667–32708, 2014

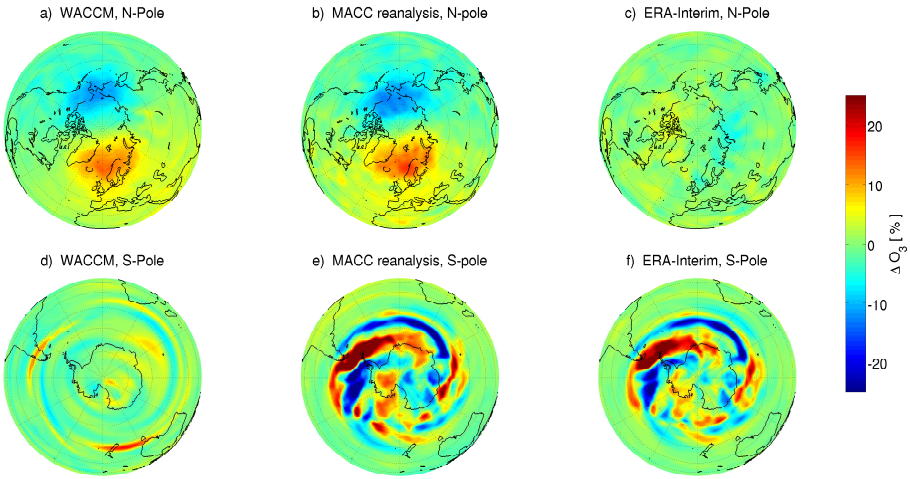

Figure 9. Relative difference of ozone VMR from 18:00 to 06:00 UT per ozone VMR at 06:00 UT. The figure shows the polar regions from the MACC reanalysis and the ERA-Interim reanalysis at 21 June 2012 and from WACCM at 5 hPa.

ACPD
14, 32667–32708, 2014

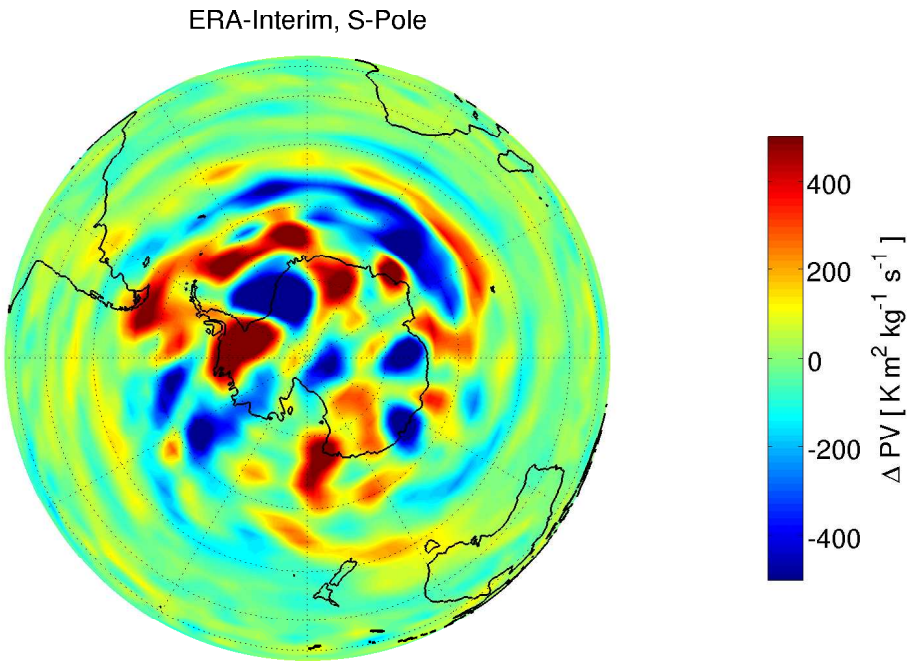

Figure 10. Difference of potential vorticity from 18:00 to 06:00 UT derived from the ERA-Interim reanalysis for 21 June 2012 in the Southern Hemisphere at 5 hPa.

ACPD
14, 32667–32708, 2014